Solid State NMR Studies of the Molecular Motions in the Polycrystalline α-L-Fucopyranose and Methyl α-L-Fucopyranoside

Y. L. Wang,[†] H. R. Tang,*[,†] and P. S. Belton[‡]

Institute of Food Research, Norwich Research Park, Norwich NR4 7UA, U.K.

Received: August 28, 2002

Molecular dynamics of polycrystalline α-L-fucopyranose and methyl α-L-fucopyranoside have been investigated using ^{13}C and ^{1}H spin relaxation times over a range of temperatures (90−400 K). For methyl α-L-fucopyranoside at 300 K, both methoxyl and methyl groups had much shorter ^{13}C T_1 than the carbons in the pyran ring. ^{13}C T_1 relaxation measurements (at 74.56 MHz) as a function of temperature enabled characterization of the 3-fold rotations of the methoxyl ($E_a \sim 9$ kJ/mol, $\tau_c \sim 0.7 \times 10^{-13}$ s) and methyl ($E_a \sim 9$ kJ/mol, $\tau_c \sim 2 \times 10^{-13}$ s) groups. Proton T_1 (100 MHz) measurements of methyl α-L-fucopyranoside showed that the relaxation processes ($E_a \sim 11$ kJ/mol, $\tau_c \sim 0.7 \times 10^{-13}$ s), corresponding to rotations of the methoxyl and methyl groups, are not distinguishable and occurred together at about 131 K. For α-L-fucopyranose, proton T_1 showed a relaxation rate maximum at 224 K, attributed to the 3-fold rotation of methyl group ($E_a \sim 15$ kJ/mol, $\tau_0 \sim 2.6 \times 10^{-13}$ s). The rotation processes of the methyl groups dominated $T_{1\rho}$ processes for both saccharides and appeared at the low-temperature end (90−150 K) of the temperature range. Contributions of hydroxyl groups to both T_1 and $T_{1\rho}$ processes were obscured by the overwhelming relaxation efficiency of methyl groups. The proton second moment showed a reduction to a lower value at about 150 K due to the rotation of methyl groups.

1. Introduction

α-L-Fucopyranose (Fuc) or 6-deoxy-α-L-mannopyranose are commonly occurring in plant polysaccharides and animal glycans, including plant cell walls,[1] brown-algal cell walls,[2] and blood plasma glycoproteins.[3] It has also been found recently in glycosphingolipids[4] and in the neutral glycopeptides from human neuroblastoma cells.[5] In plant cell walls, Fuc has been found in the side chains of rhamnogalacturonan I and in both the backbone and side chains of rhamnogalacturonan II[1]. This sugar has also been found in a carbohydrate tumor-associated antigen[6] and in the trisaccharide-protein conjugate of the phenolic glycolipid of *Mycobacterium tuberculosis*.[7]

The crystal structure of Fuc[8] and its methyl glycoside[9] (Figure 1) has been determined by X-ray diffraction. It has shown that the Fuc has an orthorhomic crystal system with the $P2_12_12_1$ space group and the unit cell has four molecules.[8] The crystal of methyl α-L-fucopyranoside (Me-Fuc) has a monoclinic lattice with space group $P2_1$ and two molecules in the unit cell.[9] Both molecules have the $^1C_4$ pyranose ring conformation and great similarity in C−H and O−H bond lengths.[8,9] Both crystals are held together in each case by an extensive three-dimensional hydrogen-bonding network.[8,9] However, they differ significantly in their hydrogen-bonding systems. For Fuc, each molecule is hydrogen-bonded to another six molecules via eight hydrogen bonds. The cyclic oxygen (O5) is involved in the hydrogen bonding as an acceptor, whereas all hydroxyl groups, except OH4, participated in the network as acceptors and donors.[8] Me-Fuc has similar conformation in both the solid state and solution and all hydroxyl groups are involved in the hydrogen bonding as donors and acceptors.[9] The molecules are arranged through a 2-fold screw axis parallel to the crystallographic axis *b*, producing a "molecular chain". Between the chains, van de Walls contacts are dominant interactions involving both CH_3 and CH_3O groups.[9] Such an arrangement is absent in the case of another 6-deoxy pyranose, methyl-α-L-rhamnopyranoside.[10]

Figure 1. Structure of Fuc and Me-Fuc.

However, there are no reports on the molecular dynamics of Fuc and its methyl glycoside in the solid state. To understand the molecular dynamics of Fuc and Me-Fuc in the solid state, we report some results for these two sugars in both protonated and deuterated crystalline forms. The methods included ^{13}C CPMAS spectroscopy, ^{13}C T_1 relaxation and proton relaxation times, T_1 and $T_{1\rho}$, and second moment M_{2r} measurements as a function of temperature. These results are interpreted in terms of their molecular motions in the solid state.

2. Experimental Section

Materials. Fuc and Me-Fuc were purchased from Sigma and used as the starting materials without further purification. For the D_2O exchanged samples, Fuc and Me-Fuc were respectively dissolved in sufficient quantity of D_2O (99.9% D) and lyophilised. The process was repeated three times to ensure that most of the exchangeable protons (hydroxyl groups) of the samples

* To whom correspondence should be addressed. Biological Chemistry, Biomedical Sciences Division, Faculty of Medicine, Imperial College of Science, Technology and Medicine, Sir Alexander Fleming Building, South Kensington, London SW7 2AZ U.K. Phone: +44 (0) 20 7594-3088. Fax: +44 (0) 20 7594-3226. E-mail: Huiru.Tang@ic.ac.uk.

† Present address: Biological Chemistry Section, Biomedical Sciences Division, Imperial College of Science, Technology and Medicine, Exhibition Road, South Kensington, London SW7 2AZ, U.K.

‡ Present address: School of Chemical Sciences, University of East Anglia, Norwich NR4 7TJ, U.K.

10.1021/jp0268617 CCC: $22.00
Published on Web 11/13/2002

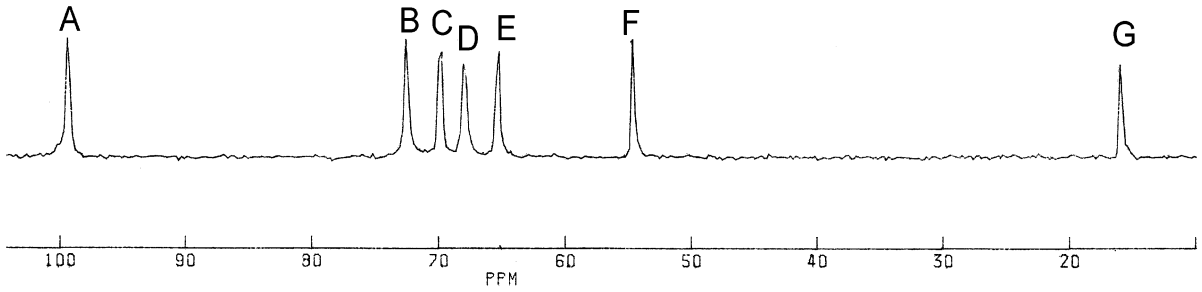

Figure 2. ^{13}C CPMAS spectrum of Me-Fuc at 300 K.

were deuterated. The samples were then crystallized from fresh D_2O in a sealed desiccator. The crystals so prepared were dried over P_2O_5 for at least 24 h *in vacco* and were sealed into 5 mm NMR tubes respectively for proton relaxation time measurements.

^{13}C CPMAS Spectroscopy. All ^{13}C CPMAS spectra were recorded on a Bruker MSL-300 spectrometer with a double-bearing magic-angle-spinning probe head (BL-7 type) operating at 300.13 MHz for proton and 74.56 MHz for carbon-13. Typically, about 220 mg sample was packed into a 7 mm Zicornia rotor with a Kel-F cap and spun at about 4 kHz. The Hartmann-Hann matching condition was set up using a polycrystalline glycine sample at 300 K. A single contact time of 1.2 ms was employed and the proton 90° pulse length was 3.6−4 μs. Glycine was used as an external reference (173.06 ppm for the carbonyl peak).

^{1}H Relaxation Time Measurements. Proton spin−lattice relaxation in the laboratory frame, T_1, in the rotating frame, $T_{1\rho}$, and second moment, M_{2r} were measured on a Bruker MSL-100 spectrometer using a 5 mm proton dedicated probe-head. The temperature was controlled with a Bruker variable temperature unit VT-3000. 10 °K increments were used and experiments were always started from the lowest temperature. A total of 15 min of waiting time after each temperature change was allowed to ensure temperature stabilization and to reach equilibrium. The sample temperature in the probe was calibrated outside the magnet and corrected accordingly.

T_1 was measured using an inversion−recovery pulse sequence [180°−τ−90°−AQ] where 90° pulse length was 1−1.5 μs. To ensure that the spread of τ values was sufficient to test for existence of multiexponential relaxation, the relaxation delay values were chosen according to[11−13] $\tau = A \times 10^{(m-1)/12}$, where A was a constant of 1−4 ms depending on the length of T_1, and m is the number of data points. The recycle delay was at least 5 times of proton T_1. A total of 48 data points were measured using single-point sampling method on the top of the FID 5 μs after the read pulse. The data were then fitted to an exponential decay function to extract T_1 values.

$T_{1\rho}$ was measured using a standard spin-locking pulse sequence [90°$_x$−τ_{SL}−AQ] where 90° pulse length was 4 μs, spin-locking delay, τ_{SL}, was between 0.4 and 40 ms depending on the length of $T_{1\rho}$. A total of 64 data points were measured using single-point sampling method on the top of the FID after the spin-lock pulse. The data were then fitted to an exponential decay function to extract $T_{1\rho}$ values.

M_{2r} was measured using the solid echo pulse sequence[14] [90°$_x$−τ_1−90°$_y$−τ−AQ] to obtain the complete Block decay signal.[15] The 90° pulse length was 1−1.5 μs, τ_1 was 12 μs and τ was chosen to be 4 μs, just slightly longer than the dead time (about 3.5 μs), to ensure observation of an echo. Dwell time was 0.5 μs, and recycle delay was 10 s. The decay part of the solid echo was fitted to a modified Gaussian function[16−18] to obtain the values of M_{2r}.

TABLE 1: ^{13}C Chemical Shift Data for Fuc and Me-Fuc from ^{13}C CPMAS Experiments

peak	A	B	C	D	E	F	G
assignment	C-1	C-4	C-3	C-2	C-5	CH_3O	CH_3
			Chemical Shifts (ppm)				
solution[a]	100.5	72.9	70.6	69.0	67.5	56.3	16.5
solid	99.6	72.7	70.1	68.2	65.3	54.7	18.2
$\Delta\delta$	−0.9	−0.2	−0.5	−0.8	−2.2	−1.6	1.7

[a] $\Delta\delta = \delta_{solid} - \delta_{solution}$; data from ref 22.

^{13}C T_1 Measurements. ^{13}C T_1 was measured using the Torchia sequence[19] over temperature range of 270−320 K. Sample temperature was calibrated in the way described in a previous publication.[20] A total of 15 relaxation delays between 0.1 and 80 s were used. A Bruker VT 1000 unit was used to control the temperature to the accuracy of 1 K. For the temperature above the ambient, normal pressurized air was used as gas source. For the low temperatures, a pressurized liquid nitrogen vessel was employed as gas source and cold nitrogen gas was used as bearing gas just as described elsewhere.[21] A total of 20 min of waiting time between each temperature change was allowed to ensure temperature stabilization and to reach equilibrium.

All relaxation time values were extracted by curve fitting using a Levenburg-Marquardt nonlinear curve-fitting routine installed in TableCurve 2D (Jandel Scientific) on a Pentium PC.

3. Results and Discussion

3.1. ^{13}C CPMAS Spectroscopy. ^{13}C CPMAS spectrum (Figure 2) of Me-Fuc showed seven clearly resolved resonances for seven carbons, respectively. The peaks at 99.6, 54.7, and 18.2 ppm are unambiguously assigned to the C-1, CH_3O, and CH_3 groups (C-6), respectively, because they are well separated from the other resonances. The remaining resonances were only assigned tentatively (Table 1) by comparison with the chemical shifts in solution state[22] because the isotropic chemical shifts in CPMAS spectra are determined to various degrees by (1) the molecular conformation in the solid state, (2) inter- and intramolecular interactions such as hydrogen bonding patterns, and (3) crystal packing in the solid state.[23−25] However, for the purpose of this study, complete and unambiguous assignments for all carbons, though ideal, are not critical as long as their signals are clearly resolved. In addition, the unambiguous assignments for C-1, CH_3O, and CH_3 groups are already sufficient for us to differentiate the ring carbons and exocyclic carbons (methyl groups). There are clear chemical-shift differences for C-1, CH_3, and CH_3O resonances in the solid state and in solution,[22] respectively (Table 1). This has been observed for monosaccharides such as, α-D-galacturonic acid[23,25] and its methyl ester,[23] α-L-rhamnopyranose monohydrate,[21,26] methyl glycosides,[21,27] and cellobiose.[17]

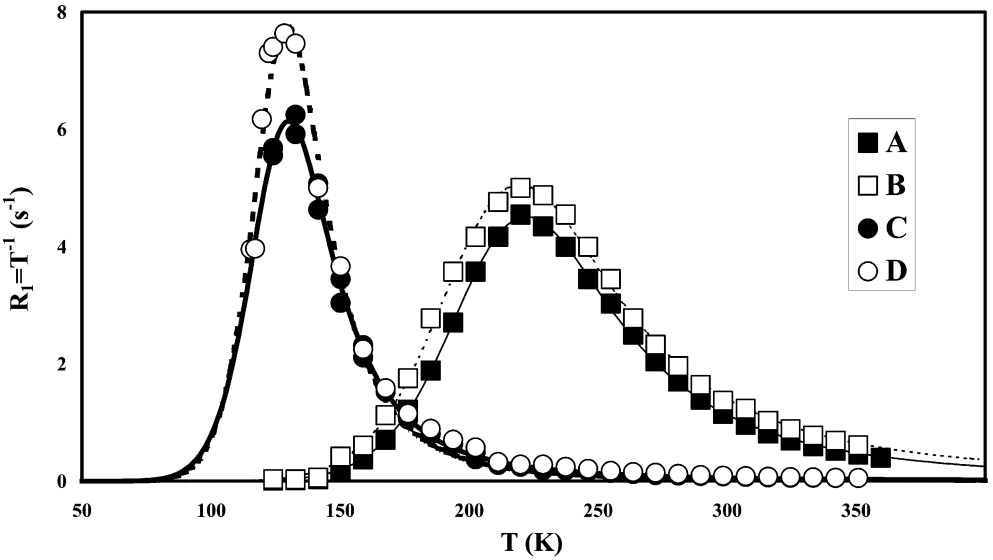

Figure 3. Temperature dependence of the proton spin−lattice relaxation rate in the laboratory frame, R_1, for Fuc and Me-Fuc. A, protonated Fuc; B, deuterated Fuc; C, protonated Me-Fuc; D, deuterated Me-Fuc; solid lines are fitted data for the protonated samples; dashed lines are fitted data for the deuterated samples.

3.2. Proton Spin−Lattice Relaxation in the Laboratory Frame. The proton spin−lattice relaxation rates, R_1, are normally measured as a function of either the strength of magnetic field or temperature to get information on the motions responsible for the relaxation. With temperature as the variable, the relaxation rate, R_1, shows a maximum (or peak) at which the motional frequency is comparable to the proton Larmor frequency. In our study, T_1 was single exponential over the temperature range of 110−360 K for Fuc and Me-Fuc in both protonated and deuterated forms. The relaxation rates, R_1, of them are shown as a function of temperature in Figure 3. For Fuc, an R_1 maximum or "relaxation peak" is observable at about 224 K, indicating the present of a motion ($\tau_c \sim 10^{-9}$ s) as an efficient proton relaxation process. Similar observations have been made for plant cell walls[16,28] and a number of sugars, such as methyl α-D-galacturonic acid methyl ester[23] and α-L-rhamnopyranoside,[21] and probably corresponds to the 3-fold rotational motion of the methyl group. Me-Fuc also showed only one peak at about 131 K, which is probably associated with the 3-fold rotational motions of methyl groups. This differs from a similar molecule, methyl α-L-rhamnopyranoside, which showed two separate peaks for methyl and methoxyl groups;[21] the peak position appeared at somewhere between them of CH_3O and CH_3 in methyl α-L-rhamnopyranoside. The peak temperature is also considerably lower than that of Fuc (224 K). This is probably due to the differences in their molecular packing and will be discussed further in later sections.

D_2O exchange of both Me-Fuc and Fuc led to an increase in the intensity of the relaxation peaks. This is owing to reduction of the number of protons to be relaxed[17,21,23] following removal of the exchangeable protons in hydroxyl groups. However, there is still only one peak observable for deuterated Me-Fuc. This peak is provisionally assigned to the motional processes of both CH_3 and CH_3O groups in this molecule. It is not possible, based on these data, to clarify whether such peak overlapping is due to the same motional characteristics for CH_3 and CH_3O groups or coincidence. Such a question can be answered by measuring properties of CH_3 and CH_3O groups in ^{13}C spectra. This is going to be discussed in a later section.

To evaluate the data quantitatively, the experimental data were fitted to the well-known Kubo-Tomita expression[11,29,30] (eq1), assuming exponential correlation functions and single rotational correlation time at a given temperature:

$$R_1 = \frac{1}{T_1} = C\left[\frac{\tau_c}{1+\omega_0^2\tau_c^2} + \frac{4\tau_c}{1+4\omega_0^2\tau_c^2}\right] \quad (1)$$

where ω_0 is the proton Larmor frequency and τ_c the rotational correlation time of the motions responsible for the spin lattice relaxation, which is assumed to follow the Arrhenius activation law

$$\tau_c = \tau_0 \exp\left(\frac{E_a}{RT}\right) \quad (2)$$

where τ_0 is the preexponential factor corresponding to the rotational correlation time at infinite temperature, E_a the activation energy, and R the gas constant. When $\omega_0\tau_c = 0.55$, R_1 reaches a peak where[18]

$$R_1^{Max} = \frac{1.76C}{\omega_0} \quad (3)$$

C in eqs 1 and 3 is the relaxation constant.

For methyl groups undergoing 3-fold rotation, C is related to the second moment (ΔM_2) modulated by the motions as described[31,32] in eq 4, assuming that the motion occurring is fast on the NMR relaxation time scale:

$$C = \frac{2}{3}\Delta M_2 \gamma^2 = \frac{27}{20N}\frac{\gamma^4\hbar^2}{r^6} \quad (4)$$

N is the total number of protons to be relaxed and, r, the mean interproton distances in the methyl group, where γ is the proton magnetogyric ratio.

For Fuc, both the protonated and deuterated samples showed satisfactory fit of the experimental data (Figure 3A,B) by the relaxation theory described in eqs 1 and 2. The motional parameters obtained from the curve fitting are tabulated in Table 2. Both E_a and τ_0 values are in accord with those for the commonly encountered methyl groups such as in amino acids[11−13,33] and in α-L-rhamnopyranose.[21]

TABLE 2: ^{1}H Relaxation Parameters for Fuc Crystals from Spin−Lattice Relaxation in the Laboratory and Rotating Frames

	Fuc (H)		Fuc (D)	
	T_1	$T_{1\rho}$	T_1	$T_{1\rho}$
relaxing groups	CH_3−C5	CH_3−C5	CH_3−C5	CH_3−C5
E_a (kJ/mol)	15.18 ± 0.08	12.0 ± 0.5[a]	13.8 ± 0.2	13.1 ± 0.4[a]
τ_0 ($\times 10^{-13}$ s)	2.64 ± 0.11	55 ± 23[a]	5.2 ± 0.4	27 ± 7.5[a]
C (10^8) rad·s^{-2}	19.87 ± 0.08	19.87[a]	22.3 ± 0.2	22.3[a]
ΔM_2 (G^2)[b]	4.17 ± 0.02	4.17	4.67 ± 0.04	4.67
r_{H-H} (Å)[c]	1.784			
R_{1max} (s^{-1})	4.5	($R_{1\rho max}$) 1511[a]	5.0	($R_{1\rho max}$) 1787[a]
temp. at R_{1max} (K)	224	($R_{1\rho max}$) 120[a]	224	($R_{1\rho max}$) 122[a]

[a] Values obtained from curve-fitting spin lattice relaxation data. Values obtained from fitting $T_{1\rho}$ data with C values contrained to these from T_1 data. [b] Second moment modulated by the motions calculated according to eq 4. [c] Average C−H bond length from the ^{1}H T_1 data (see text for details).

TABLE 3: ^{1}H Relaxation Parameters for Polycrystalline Me-Fuc from Spin−Lattice Relaxation in the Laboratory and Rotating Frames

	Me-Fuc (H)		Me-Fuc (D)	
	T_1	$T_{1\rho}$	T_1	$T_{1\rho}$
	CH_3OC^1 & CH_3−C^5H	CH_3OC^1 & CH_3−C^5H	CH_3OC^1 & CH_3−C^5H	CH_3OC^1 & CH_3−C^5H
experimental values				
E_a (kJ/mol)	10.36 ± 0.14	12.94 ± 0.80[a]	11.70 ± 0.37	10.80 ± 0.34[a]
τ_0 ($\times 10^{-13}$ s)	0.68 ± 0.08	0.15 ± 0.10[a]	0.19 ± 0.06	0.66 ± 0.20[a]
C (10^8) rad·s^{-2}	27.05 ± 0.20	27.05[a]	34.22 ± 0.71	34.22[a]
ΔM_2 (G^2)[b]	5.67 ± 0.04	5.67	7.17 ± 0.15	7.17
r_{H-H} (Å)[c]	1.854 ± 0.014			
R_{1max} (s^{-1})	6.13	($R_{1\rho max}$) 2029[a]	7.7	($R_{1\rho max}$) 2520[a]
temp. at R_{1max} (K)	131	($R_{1\rho max}$) 86[a]	130	($R_{1\rho max}$) 78[a]

[a] Values obtained from curve-fitting spin lattice relaxation data. Values obtained from fitting $T_{1\rho}$ data with C values contrained to these from T_1 data. [b] Second moment modulated by the motions calculated according to eq 4. [c] Average C−H bond length from the ^{1}H T_1 data (see text for details).

The X-ray structure reported[8] that the interproton distances in the methyl group were 1.530, 1.510, and 0.939 Å. These are much shorter than the values in a similar molecule, α-L-rhamnopyranose,[34] and in commonly encountered methyl groups in amino acids.[33,35] Two of the values are smaller than the corresponding value in the water of crystallization in α-L-rhamnopyranose monohydrate[34] (1.522 Å). One of them (0.939 Å) is even shorter than the C−H bond length (0.96 Å) in the same molecule.[8] Inaccurate proton position in the X-ray structure is a well-known problem. Without neutron scattering data, NMR relaxation may offer a good opportunity to measure the mean H−H distance as pointed out previously[33] (eq 4).

For the protonated Fuc, the measured C from T_1 data is 19.87 $\times$ 10^8 s^{-2}. With eq 4, this gives a mean r_{H-H} of 1.784 Å, which is in excellent agreement with the values in amino acids[33,35] and α-L-rhamnopyranose monohydrate.[34] For the deuterated Fuc, C value was obtained from the T_1 data as 22.27 $\times$ 10^8 s^{-2}. Assuming that the D_2O exchange does not affect the distances between the nonexchangeable protons, the experimental C value gives a calculated N value of 10−11 taking r_{H-H} as 1.784 Å. Therefore, this observation implies that one or two protons were not D_2O exchanged.

For Me-Fuc, fitting the T_1 data to eqs 1 and 2 showed good agreement between the experimental and predicted values (Figure 3C,D). The relaxation parameters (E_a, τ_0) obtained (Table 3) are in accord with those for the methyl groups. The experimental C values (27.05 $\times$ 10^8 s^{-2}) for the protonated methyl Fuc and (34.22 $\times$ 10^8 s^{-2}) in deuterated sample are much greater than these for CH_3 or CH_3O alone, providing further evidence that the R_1 maxima for CH_3 or CH_3O groups are overlapped. This is discussed further in later section with ^{13}C data.

X-ray structure[9] showed that the interproton distances in the CH_3O group were 1.463, 1.360, and 1.443 Å; they are 1.540, 1.665, and 1.503 Å in the CH_3 group. Most of these again are even shorter than that of water in α-L-rhamnopyranose monohydrate,[34] indicating unreliable measurement of hydrogen positions in X-ray structure. The experimental C values for CH_3 and CH_3O groups (27.05 $\times$ 10^8 s^{-2}) in the protonated methyl Fuc give a mean r_{H-H} of 1.854 Å in these two groups.

The motions of the exchangeable protons, namely, OHs, have also been shown to be the proton relaxation pathways in sugars such as glucopyranose,[36] methyl glycosides,[21,31,32] α-D-galacturonic acid,[23] α-L-rhamnopyranose,[21] and cellobiose.[17] For the present two sugars, there were no corresponding R_1 peaks observed. This is due to the fact that hydroxyl groups in sugars generally provide a weak relaxation process with a C value in the order of 10^7 s^{-2} and an E_a value of 10−20 kJ/mol.[31,32,36] Under our experimental conditions, the R_1 maximum from hydroxyl groups is expected to appear at about 300−320 K with a value of 0.03 s^{-1}(eq 3). However, at 320 K, the R_1 contribution from methyl groups is about 0.7−0.8 s^{-1} for Fuc and about 0.1 s^{-1} for Me-Fuc. Therefore, the small R_1 peaks of OH groups are expected obscured.

3.3. Proton Spin−Lattice Relaxation in the Rotating Frame. The relaxation rate $R_{1\rho}$ of Fuc and Me-Fuc as a function of temperature is shown in Figure 4. Both saccharides showed only one relaxation process (Figure 4) at T < 170 K although these peaks have not reached their maxima. However, there is no motion of the hydroxyl groups observed.

To analyze the $R_{1\rho}$ data further, the experimental values were fitted to an expression similar to that used in R_1 analysis:[11−13,30]

$$R_{1\rho} = \frac{1}{T_{1\rho}} = \frac{3}{2}C\left[\frac{\tau_c}{1+4\omega_e^2\tau_c^2} + \frac{5}{3}\frac{\tau_c}{1+\omega_0^2\tau_c^2} + \frac{2}{3}\frac{\tau_c}{1+4\omega_0^2\tau_c^2}\right] \quad (5)$$

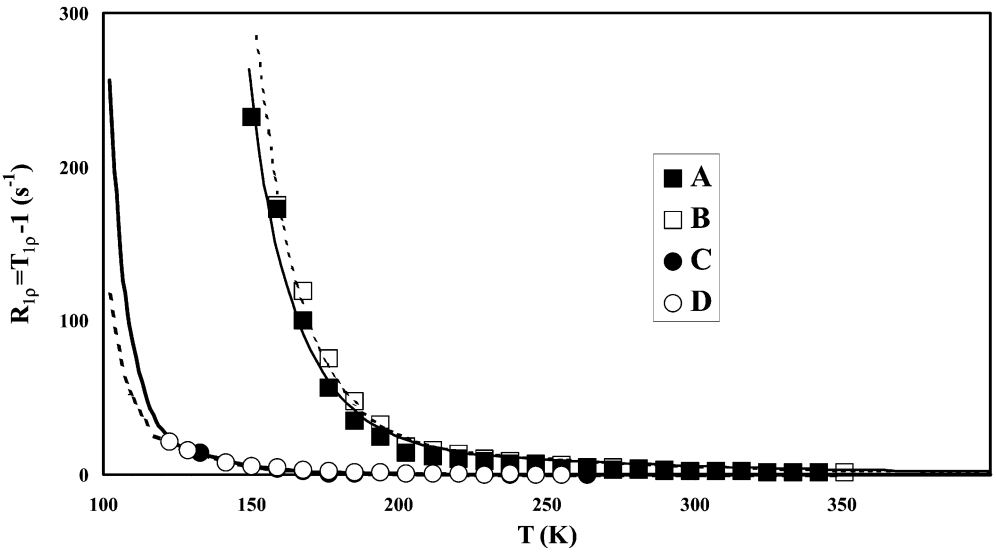

Figure 4. Temperature dependence of the proton spin−lattice relaxation rate in the rotating frame, $R_{1\rho}$, for Fuc and Me-Fuc. A, protonated Fuc; B, deuterated Fuc; C, protonated Me-Fuc; D, deuterated Me-Fuc; solid lines are fitted data for the protonated samples; dashed lines are fitted data for the deuterated samples.

where ω_0, τ_c, and C have the same meaning as in eq 1. ω_e is the effective field for relaxation in frequency units, which is often dependent on the spin-locking frequency, ω_{SP}, and the local dipolar field (in frequency unit), ω_L.

In the current situation, ω_{SP} and ω_L are in the same order of magnitude (about 67 and 40 kHz respectively), around the relaxation maximum, $\omega_e\tau_c = 0.55$, hence $\tau_c \leq T_2$. The effects of the local dipolar field have therefore been taken into consideration by the McCall-Douglass equation[37]

$$\omega_e = \sqrt{\omega_{SP}{}^2 + \omega_L{}^2} \tag{6}$$

The temperature dependence of ω_L was modeled satisfactorily by a Sigmoid function[11−13] for both the protonated and deuterated samples respectively to give the closest values to that of the experimental ones within the temperature range we used.

$R_{1\rho}$ data for the protonated and deuterated Fuc and Me-Fuc were fitted to eqs 5 and 6. For both sugars, the C values were constrained to the values for the methyl group obtained from the T_1 experiments. Parameters obtained are tabulated in Tables 2 and 3. The E_a values (10−13 kJ/mol) for the relaxation processes agree well with that of the methyl group rotation.

3.4. ^{13}C Spin−Lattice Relaxation of Me-Fuc in the Laboratory Frame (T_1). At the room temperature, ^{13}C T_1 was much shorter for CH_3O and CH_3 groups than the ring carbons as in the case of methyl α-L-rhamnopyranose.[21] This is due to the fast motions of these two groups. We measured the ^{13}C T_1 for each carbon of Me-Fuc over the temperature range of 270−320 K at the ^{13}C frequency of 74.56 MHz. In the solid state, the ^{13}C T_1, for those carbons attached with protons, is normally dominated by the H−C heteronuclear dipolar interaction and can be expressed as[30]

$$\frac{1}{T_1} = \boldsymbol{k}\left[\frac{\tau_c}{1+(\omega_p-\omega_c)^2\tau_c{}^2} + \frac{3\tau_c}{1+\omega_c{}^2\tau_c{}^2} + \frac{6\tau_c}{1+(\omega_p+\omega_c)^2\tau_c{}^2}\right] \tag{7}$$

where ω_P and ω_C are the Larmor frequency for ^{1}H and ^{13}C, respectively.

Assuming that all of the methyl groups are undergoing 3-fold rotation and have the same correlation time, relaxation constant, $\boldsymbol{k}$, can be expressed as[30] in eq 8:

$$\boldsymbol{k} = \frac{3}{10}\left(\frac{\mu_0}{4\pi}\right)^2 \gamma_p{}^2\gamma_c{}^2\hbar^2 r_{pc}{}^{-6} \tag{8}$$

where r_{pc} is the mean C−H bond length and γ_P and γ_C are the magnetogyric ratios for ^{1}H and ^{13}C. As discussed earlier, the hydrogen positions in the X-ray structure of Me-Fuc was not reliable, so we take the values measured in proton T_1 experiments. Assuming the methyl groups adopt perfect tetrahedral geometry, the calculated C−H length is 1.136 Å. This gives the calculated $\boldsymbol{k}$ value of 5.03×10^9 s^{-2}. As shown in T_1 data, τ_c of methyl groups in Me-Fuc is in the order of nanosecond ($\sim 10^{-9}$ s) at about 130 K, the "extreme narrowing" condition ($\omega_o\tau_c \ll 1$)[30] applies at 270−320 K (74.56 MHz), hence combination of eqs 7 and 8 gives

$$\frac{1}{T_1} = 10\,\boldsymbol{k}\tau_0 e^{(E_a/RT)} = 5.03 \times 10^{10}\,\tau_0 e^{(E_a/RT)} \tag{9}$$

and a logarithmic plot of T_1 vs $1/T$ is linear. The results of such a plot are shown in Figure 5 and justify the model used. Treating E_a and τ_0 as variable parameters, best fits of the ^{13}C T_1 data for methoxyl and methyl groups to eq 9 yield the results in Table 4 and shown as solid lines in Figure 5.

The τ_0 value for CH_3O ($\sim 0.7 \times 10^{-13}$ s) groups is in accord to the values for CH_3O ($(0.9-9) \times 10^{-13}$ s) in methyl α-D-galacturonic acid methyl ester[23] and methyl glycosides;[21,31,32] the τ_0 value for CH_3 ($\sim 2 \times 10^{-13}$ s) agrees with that for CH_3 (2×10^{-13} s) in a structurally similar molecule, methyl α-L-rhamnopyranoside.[21] The E_a ($\sim$9 kJ/mol) for both CH_3O and CH_3 groups, however, are slightly lower than that in methyl α-L-rhamnopyranoside (12−13 kJ/mol)[21] measured from proton relaxation data even though they are in the right range for CH_3O (4−10 kJ/mol) in methyl glycosides[31,32] or for CH_3 (9−17 kJ/mol) in amino acids[11−13,33] measured from proton relaxation data. Nevertheless, the discrepancy may result from the fact that (1) the molecular packing in Me-Fuc crystals[9] is considerably different from that of methyl α-L-rhamnopyranoside and (2) these data were measured with an approximation highlighted in eq 9.

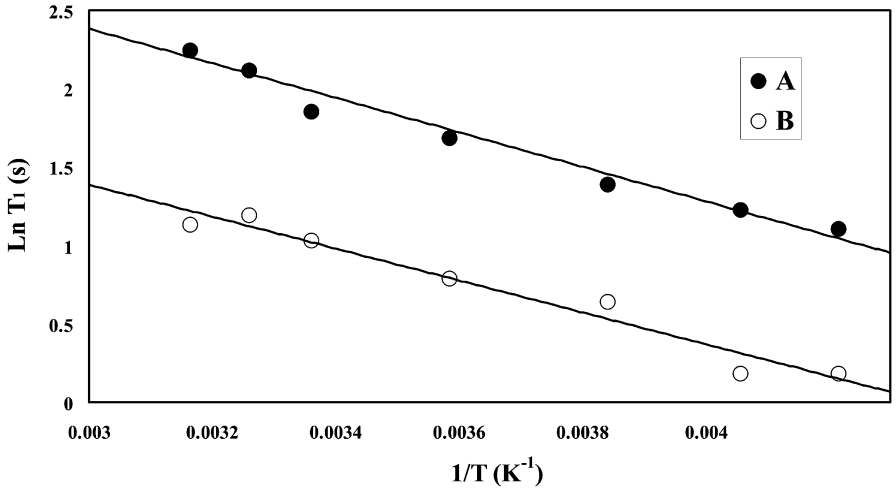

Figure 5. Temperature dependence of the ^{13}C spin−lattice relaxation time in the laboratory frame for the methoxyl and methyl groups of Me-Fuc. A, $^{6}CH_3{}^{5}CH$; B, CH_3O; solid lines are fitted data.

TABLE 4: ^{13}C T_1 Relaxation Parameters for Polycrystalline Me-Fuc

relaxing groups	CH_3OC^1	CH_3-C^5H
r_{pc} (Å)	1.136[a]	1.136[a]
calculated $\boldsymbol{k}$ (10^9 rad·s^{-2})	50.3	50.3
E_a (kJ/mol)	9.14 ± 0.45	8.45 ± 0.77
τ_0 ($\times 10^{-13}$ s)	0.678 ± 0.04	2.34 ± 0.13

[a] Average C−H bond length in CH_3 and CH_3O groups is taken from ^1H T_1 data (see text for details).

In interpreting the proton data, we proposed that the R_1 maxima for CH_3O and CH_3 were overlapped. However, τ_0 values obtained from ^{13}C data differ considerably for the CH_3 and CH_3O groups though the E_a values were similar within the margin of error. This implies that the motions of these two groups are different and the motion-induced R_1 maxima appeared at the same temperature only by coincidence. The different behaviors of this sugar from that of methyl α-L-rhamnopyanoside,[21] a chemically similar molecule, is probably due to the differences in the molecular packing; methoxyl groups in this molecule are engaged in an extensive hydrophobic interaction network.[9]

To support this point further, we predicted the R_1 maxima in ^1H NMR using the relaxation parameters obtained from ^{13}C data (Table 4); they are at 104 and 109 K for methoxyl and methyl groups, respectively. Although this is at lower temperature than observed (Figure 3), this does explain the failure to show two peaks. This also provides supportive evidence to the conclusion that CH_3 and CH_3O groups had different motional properties, their relaxation maxima overlapped only coincidentally and appeared as one peak in ^1H T_1 experiment (Figure 3C&D).

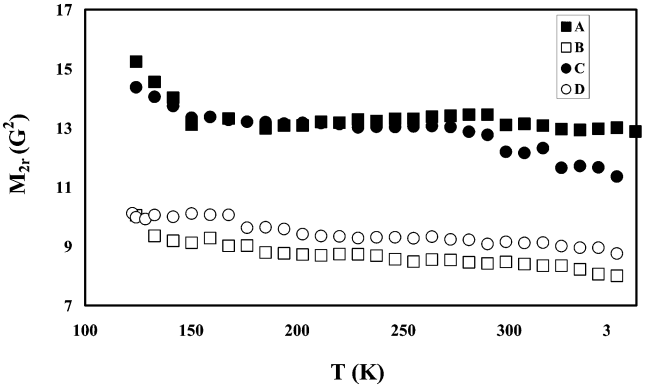

Figure 6. Temperature dependence of the proton second moment, M_{2r}, for Fuc and Me-Fuc. A, protonated Fuc; B, deuterated Fuc; C, protonated Me-Fuc; D, deuterated Me-Fuc.

3.5. Proton Second Moment. The free induction decay (FID) of both Fuc and Me-Fuc cannot be described either in a single Gaussian or exponential decay function. They can be better approximated to a modified Gaussian function[18] (eq 10) as in the cases of plant cell walls[16,28] and galacturonic acid or its methyl ester.[23]

$$I(t) = I_0 \exp\left(\frac{-a^2t^2}{2}\right)\frac{\sin bt}{bt} \qquad (10)$$

The residual second moment can be used to evaluate FID as defined $M_{2r} = a^2 + b^2/3$.

TABLE 5: Proton Second Moment M_{2r} Data for Fuc and Me-Fuc

	Me-Fuc(H)	Me-Fuc(D)	Fuc (H)	Fuc (D)
		Measured Plateau Values		
first plateau (G^2)	13.2 ± 0.2 (150−270 K)	9.5 ± 0.3 (150−350 K)	13.2 ± 0.2 (150−350 K)	8.5 ± 0.5 (150−350 K)
		M_{2r} Reduction		
first reduction	T < 150 K	T < 150 K	T < 150 K	T < 150 K
second reduction	T > 300 K			
		Calculate M_2 (G^2)		
rigid lattice M_2	18.9[a]	16.7[a]	17.4[a]	13.2[a]
after CH_3 motion	13.2	9.5	13.2	8.5
after OHs motion	13.0		13.0	

[a] Calculated values from the value of the first plateau and ΔM_2 in Tables 2 and 3.

In general, M_{2r} is expected to decrease when the motional correlation time τ_c is comparable to the inverse of line−width, i.e.

$$\tau_c = (\gamma\sqrt{M_{2r}})^{-1} \quad (11)$$

The line narrowing transition is expected to be complete when $(\gamma M_{2r}^{1/2})t_c \ll 1$.

Temperature dependence of M_{2r} for the protonated/deuterated Fuc and its methyl ether is shown in Figure 6. For the protonated saccharides, an M_{2r} reduction and a plateau are observable at about 150 K and $T > 150$ K (13.2 G^2), respectively. The reduction is associated with the modulation of the methyl groups' rotation. Because the reliable data for the interproton distances in their structure are not available, their rigid lattice M_{2rigid} values cannot be calculated from the lattice summation. However, with the experimental values of the plateau at 150−300 K, ΔM_2 in Tables 2 and 3 and eq 4, their rigid lattice M_{2r} were calculated and tabulated in Table 5. There appears an M_{2r} reduction at about 300 K for the protonated samples, which may be attributable to the motional effect of hydroxyl groups. However, no quantitative analysis of the data is attempted because the M_{2r} reduction from the motions of hydroxyl groups is expected to be in the order of 0.2−0.3 G^2, which is comparable with the margin of error.

For the deuterated samples, the M_{2r} values are much smaller than these for their protonated forms. This can be explained by the reduction of (proton) spin density after removal of exchangeable protons. The M_{2r} reduction, owing to the methyl rotation, for these two samples appeared to complete at $T < 150$ K.

4. Conclusion

The major relaxation pathways in Fuc and its methyl ether are the 3-fold rotation of CH_3O and CH_3 groups. For Me-Fuc, the motional properties of methoxyl and methyl groups were different but the induced relaxation maxima coincided at the same temperature, thus are not clearly distinguishable in proton T_1 experiments. This was further confirmed by the ^{13}C T_1 data. The motions of methyl groups dominated the second moment changes. Sugar ring puckering motions were not detectable in the solid state.

Acknowledgment. BBSRC is acknowledged for a Competitive Strategic Grant. Dr. David Hughes at John Innes Centre is acknowledged for his helpful advice and discussion on the X-ray structures of α-L-fucopyranose and methyl α-L-fucopyranoside. Dr. Olaf Beckonert at Imperial College is acknowledged for his help in reading the French ref 8.

References and Notes

(1) Brett, C. T.; Waldron, K. W. *The Physiology and Biochemistry of Plant Cell Walls*; Unwin Hyman: London, 1990.
(2) Mackie, W.; Preston, R. D. *Algal Physiology and Biochemistry*; Stewart, W. D. P., Ed.; Blackwell: London, 1974; pp 40−85.
(3) Kennedy, J. F.; White, C. A. *Bioactive Carbohydrates in Chemistry, Biochemistry and Biology*; Ellis Harwood: Chichester, U.K., 1983; pp 182−227.
(4) Norberg, T.; Walding, M. *Glycoconjugate J.* **1988**, *5*, 137−143.
(5) Santer, U. V.; Glick, M. C.; Vanhalbeek, H.; Vliegenthart, J. F. G. *Carbohydr. Res.* **1983**, *120*, 197−213.
(6) Diakun, K. R.; Matta, K. L. *J. Immunol.* **1989**, *142*, 2037−2040.
(7) Aspinall, G. O.; Khare, N. K.; Sood, R. K.; Chatterjee, D.; Rivoire, B.; Brennan, P. J. *Carbohydr. Res.* **1991**, *216*, 357−373.
(8) Longchambon, P. F.; Ohannessian, J.; Neuman, D. A. A. *Acta Crystallogr. Sec. B* **1975**, *31*, 2623−2627.
(9) Lamba, D.; Segre, A. L.; Fabrizi, G.; Matsuhiro, B. *Carbohydr. Res.* **1993**, *243*, 217−224.
(10) Shalaby, M. A.; Fronczek, F. R.; Younathan, E. S. *Carbohydr. Res.* **1994**, *258*, 267−274.
(11) Belton, P.; Wang, Y. L. *Mol. Phys.* **1997**, 90, 119−125.
(12) Wang, Y. L.; Belton, P. S.; Tang, H. R. *Chem. Phys. Lett.* **1997**, *268*, 387−392.
(13) Wang, Y. L.; Belton, P. S.; Tang, H. R. *Solid State NMR* **1999**, *14*, 19−32.
(14) Powles, J. G.; Mansfield, P. *Phys. Lett.* **1962**, 2, 58−59.
(15) Powles, J. G.; Strange, J. H. *Proc. Phys. Soc.* **1963**, *82*, 6−15.
(16) Tang, H. R.; Zhao, B. L.; Belton, P. S.; Sutcliffe, L. H.; Ng, A. *Magn. Reson. Chem.* **2000**, *38*, 765−770.
(17) Tang, H. R.; Belton, P. S. *Solid State NMR* **2002**, *21*, 117−133.
(18) Abragam, A. *The Principles of Nuclear Magnetism*; Oxford University Press: New York, 1961.
(19) Torchia, D. A. *J. Magn. Reson.* **1978**, *30*, 613−615.
(20) Riddell, F. G.; Spark, R. A.; Gunther, G. V. *Magn. Reson. Chem.* **1996**, *34*, 824−828.
(21) Tang, H. R.; Wang, Y. L.; Belton, P. S. Submitted for publication.
(22) Bock, K.; Pedersen, C. *Adv. Carbohydr. Chem. Biochem.* **1983**, *41*, 27−65.
(23) Tang, H. R.; Belton, P. S. *Solid State NMR* **1998**, *12*, 21−30.
(24) Sastry, D. L.; Takegoshi, K.; Mcdowell, C. A. *Carbohydr. Res.* **1987**, *165*, 161−171.
(25) Tang, H. R.; Belton, P. S.; Davies, S. C.; Hughes, D. L. *Carbohydr. Res.* **2001**, *330*, 391−399.
(26) Liu, F.; Phung, C. G.; Alderman, D. W.; Grant, D. M. *J. Magn. Reson. A* **1996**, 120, 242−248.
(27) Liu, F.; Phung, C. G.; Alderman, D. W.; Grant, D. M. *J. Am. Chem. Soc.* **1996**, *118*, 10629−10634.
(28) Tang, H. R.; Belton, P. S. Proton relaxation in plant cell walls and model systems. In *Advances of Magnetic Resonance in Food Science*; Belton, P. S., Hills, B. P., Webb, G. A., Eds.; RSC: Cambridge, 1999; pp 166−184.
(29) Kubo, R.; Tomita, K. *J. Phys. Soc. Jpn.* **1954**, *9*, 888−919.
(30) Harris, R. K. *Nuclear Magnetic Resonance Spectroscopy*; Pitman Books Ltd: London, 1983.
(31) Latanowicz, L.; Reynhardt, E. C.; Utrecht, R.; Medycki, W. *Ber. Bunsen-Gesell. Phys. Chem. Chem. Phys.* **1995**, *99*, 152−157.
(32) Reynhardt, E. C.; Latanowicz, L. *Chem. Phys. Lett.* **1996**, 251, 235−241.
(33) Andrew, E. R.; Hinshaw, W. S.; Hutchins, M. G.; Sjoblom, R. O.; Canepa, P. C. *Mol. Phys.* **1976**, *32* (3), 795−806.
(34) Takagi, S.; Jeffrey, G. A. *Acta Crystallogr. Sec. B* **1978**, *34*, 2551−2555.
(35) Wang, Y. L.; Belton, P. S.; Tang, H. R.; Wellner, N.; Davies, S. C.; Hughes, D. L. *J. Chem. Soc. Perkin 2* **1997**, 899−904.
(36) Latanowicz, L.; Reynhardt, E. C. *Ber. Bunsen Gesell. Phys. Chem. Int. J. Phys. Chem.* **1994**, *98*, 818−823.
(37) McCall, D. W.; Douglass, D. C. *Appl. Phys. Lett.* **1965**, *7*, 12−14.